Experimental Studies of a Linear Strip Cesium Contact Ion Thruster

G. Eschard,* A. Pelissier,† J. Paulin,† J.F. Bonnal‡
Laboratoires d'Electronique et de Physique appliquee, Limeil-Brevannes, France

A cesium contact ion thruster has been developed and the techniques employed for the construction are described. The thrust (1.4 mN), ion current density (7mA/cm^2), beam divergence (17°), deflection capability (±5°) and other working characteristics are found to be in good agreement with the theoretical calculations and the required performances. From separate tests of the different components of the thruster, the lifetime is estimated well above the necessary 15,000 hr. A general understanding of the physics of the drain currents on the accelerator electrodes is obtained by experimental comparisons between different regimes of the same thruster. Thermoionic electron emission enhanced by Schottky effect and cold emission are the main causes of these losses and their suppression seems possible by only slight modifications in the design of the electrodes.

Nomenclature

I_F = beam current
I_A = accelerator electrodes current
J = electron current density emitted from the accel. electrodes
V_i = ionizer voltage
V_A = accelerator voltage
V = $V_i + V_A$ total voltage across accelerator gap
E = electric field at the accelerator electrodes surface
ϕ = work function of a cesiated surface
θ_i = ionizer temperature
θ_A = accelerator electrodes temperature
η_u = propellant efficiency
τ^* = $1-\eta_u$ = cesium flow in the simulated regime normalized to the corresponding flow in the nominal regime.
φ = thrust vectoring angle
e = electronic charge
K = Boltzmann constant
ϵ_0 = vacuum dielectric constant

Introduction

CESIUM contact ion thrusters have been extensively studies in the recent years[1] They can be scaled over a wide range of thrust levels and are capable of high propellant efficiency and long lifetime. The general objective of the work described here is the development of such a thruster to be integrated in a geostationary telecommunications satellite.[2,3]

The basic studies of the different components have already been discussed[4,5] The technology of the porous tungsten is now in hand (metallurgy, welding...) and two possible materials have been selected for further development: a spherical tungsten powder and a thoriated tungsten.[6] A new method used for the calculation of the ion optics based on a parametric study permits an optimal choice of the shape and voltage of the electrodes.[4] For the selected geometry, the ion current is 6.5 mA/cm^2 and the ion beam divergence is ±17.5°. Tests of neutralizers showed that the behavior of carburized thoriated tungsten filaments (WThC) or lanthanum hexaboride wires (LaB_6) under ion bombardment was acceptable.

During these preliminary tests, the performances of the main components were extensively studied. Their lifetime expectations were deduced and are summarized in Table I. As a consequence of these studies, the decision was taken to build an engineering model of the thruster. The present paper describes the techniques employed for its construction and analyses the main results obtained during its experimentation.

Description of the Thruster

The basic requirements are the achievement of a thrust of 1.5 mN at a specific impulse of 6,700 sec. Figure 1 gives a cross section of the thruster. To obtain a compact thruster which can be easily integrated into the propulsion subsystem, a rigid plate located at the rear of the motor serves as a base which supports all the components and the electrical connections. The ionizer assembly is a porous tungsten linear strip 51 mm long by 5.8 mm wide. The emitting surface is concave (r = 5 mm). It is electron beam welded on a molybdenum support in which the heaters are introduced.

The heat transfer is based on conduction in order to reduce the working temperature and to increase the lifetime of the heaters. These heaters are made of alumina coated tungsten wire, wound in a spiral, and introduced intoi an alumina tube. The extremities of the filament are spot welded on small cylinders of tantalum fitted on the alumina tubes, allowing a good thermal and mechanical independence between the filament and its connections.

The results of the thermal tests are already mentioned in Table 1. An ionizer was heated at 1300° C during 2,700 hr with only one filament working at 4 times its nominal power. During the 2,000 cycles, the ionizer temperature was varied

Table 1 Experimental results related to thruster lifetime

$\eta_u > 99\%$	→ Theoretical life-time of the ion optics >20,000 hr
Sintering of the ionizer negligible after a 4,700 hr test	→ Expected life-time of the ionizer >15,000 hr
Heaters of the ionizer Tests at 4 times the nominal power	→ No evolution after: 2,700 hr D.C. 2,000 hr cycled
Neutralizer filaments test without ion bombardment	→ Expected lifetime: >40,000 hr (WThC) >10,000 hr (LaB_6)
Test with high current density bombardment	

Presented as Paper 75-412 at the AIAA 11th Electric Propulsion Conference, New Orleans, Louisiana, March 19-21, 1975; submitted May 8, 1975; revision received August 25, 1975. This research was performed under contracts from the Societe Europeenne de Propulsion and the Centre National d'Etudes Spatiales and in collaboration with ONERA.

Index categories: Electric and Advanced Space Propulsion; Spacecraft Attitude Dynamics and Control.

†Division Head.
†Physicist.
‡Consultant.

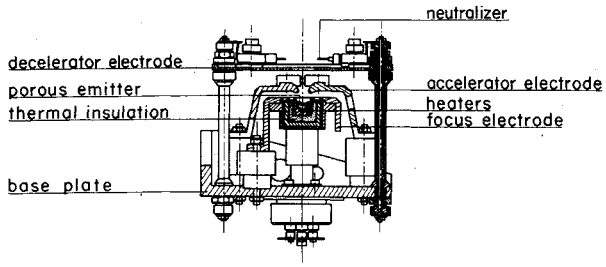

Fig. 1 Cross section of the thruster module.

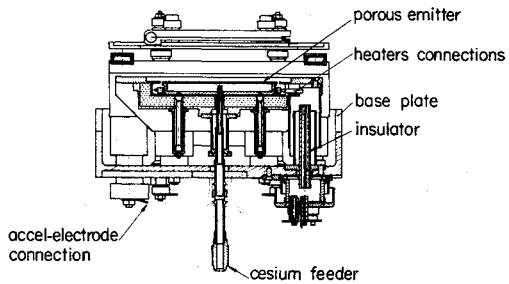

Fig. 2 Longitudinal section of the thruster.

between 250 and 1150°C every 15 min. One heater being able to provide alone the nominal power, there is a possibility of redundancy of this function.

The accelerator and decelerator electrodes are in copper. The two halves of the accelerator are insulated separately in order to permit the deflection of the beam by differential polarization. Great care was taken in the design of the high-voltage insulators. All of them are fixed on the base plate and protected by metallic caps; so the alumina is never in direct view of the ionizer and of the cesium vapor flow. When electrical connections are needed (polarization or heaters), the wires are placed inside the insulator and the connections are placed on the backside of the base plate as can be seen on Fig. 2. One can also see on this figure the cesium duct and the thermal shield assembly around the ionizer.

One should have in mind that, in order to simplify the construction and decrease the cost of the model, no effort was made to optimize the weight of the accessory parts. But the present size ($110 \times 80 \times 85$ mm) can be regarded as close to the optimum. The most important cause of power consumption is the radiation emitted by the front face of the ionizer. However, the losses from the side and rear faces must be minimized. The analysis of the conditions of heat transfer by radiation and conduction between successive metallic screens in vacuum led to the design of a multiple-foil thermal insulation. The shields are made of about 50 molybdenum sheets 25μ thick, pressed together with insulation provided by zirconia powder; the mean size of the zirconia grains is 10μ.

The measured coefficient of thermal conductivity is plotted on Fig. 3 vs the temperature. A gain greater than 10 is obtained when compared with the conductivity of the best conventional insulating materials. Another advantage of this technique is the good behavior of the complete ionizer assembly against vibrations and thermal stresses. The experimental result obtained is a decrease to a minimum of the thermal losses from the ionizer which are the main cause of the high-power consumption of a cesium contact thruster. In the present case, the total power necessary to heat the ionizer at 1100°C is 39 W, 25 W being lost on the front face and only 14 through the shields and the supports and connections. These experimental values are in good agreement with the calculated losses from the different components: 5 W by radiation from the shields, and 9 W by conduction through the cesium feeder, supports, and connections.

Experimental Study of the Thruster

The aim of the laboratory tests to be discussed here is to compare the actual performance of the thruster to that

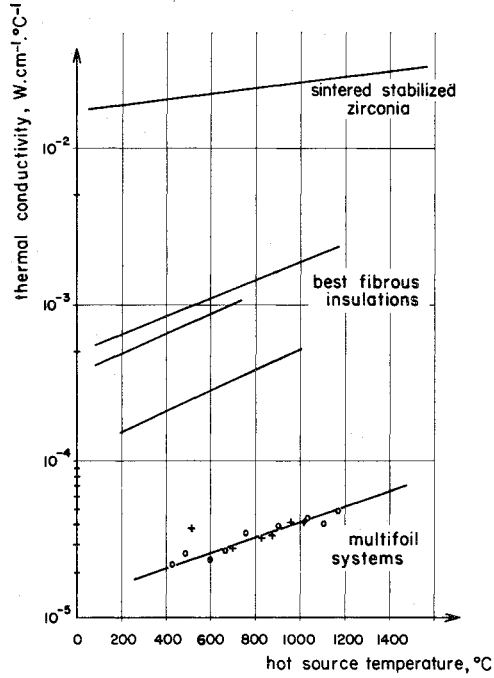

Fig. 3 Thermal conductivity of different insulations.

required. They do not include long duration tests which are performed elsewhere on a similar engine. All the experiments were done in a vacuum tank equipped with ion and getter pumps which minimize the presence of oxygen in the residual atmosphere.[7] The liquid nitrogen cooled trap worked continuously during the tests and the base pressure was in the 10^{-8} Torr range. Table 2 compares the planned performances as defined in the CNES project with typical experimental results obtained during the laboratory tests and on the whole the figures in the two columns are in good agreement.

A comprehensive study of the working conditions of the thruster led to the choice of an optimal set of beam parameters. A typical experiment is summarized in Fig. 4 where the extracted current density is plotted against the total extraction voltage for different values of the beam and accelerator voltages. From these measurements, the accelerator voltage was fixed at −3,500 volts. This improved the extracted current density from the 6.5 mA/cm^2 planned value to

Table 2 Comparison between planned and measured performances

	Planned	Experimental
Thrust (mN)	1.5	1.37[a]
Specific impulse (s)	6,700	6,700
Propellant efficiency %	≥99	≃99
Beam divergence (°)	17.5	17[b]
Beam voltage (V)	3,000	3,000
Beam current (mA)	16.5	15.1[a]
Accelerating voltage (V)	−3,000	−3,500
Accelerator current (mA)	min	1.45[c]
Decelerator current (mA)	min.	0.02
Ionizer current (mA)	16.5	16.5
Ionizer current density (mA/cm^2)	6.5	7.0
Ionizer temperature (°C)	1100	1200
Beam power (W)	49.5	45.3
Ionizer heating power (W)	37 at 1100°C	39 at 1100°C 50 at 1200°C
Other power losses (drain currents) (W)	≤3	9.5
Power consumption of the thruster (without neutralizer and vaporizer)	89.5	92 at 1100°C 105 at 1200°C

[a]Depends on the effective surface of the ionizer for a given current density; b) 17° includes 90% of the beam; [c]Stable for 60 hr.

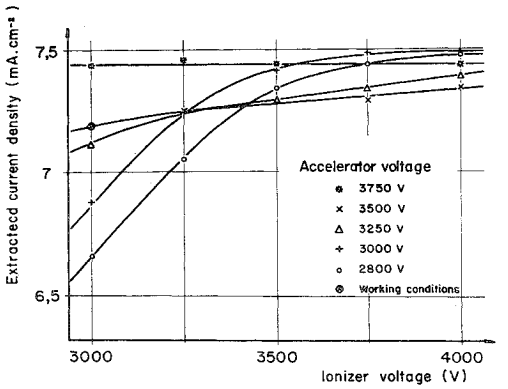

Fig. 4 Variation of the extracted current density with ionizer and accelerator voltages.

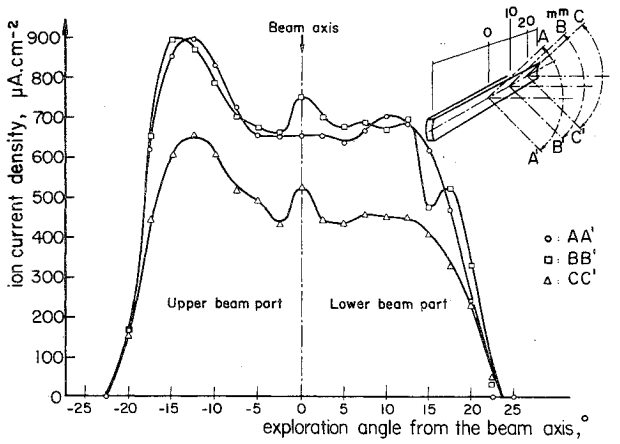

Fig. 5 Radial exploration of the beam.

7 mA/cm^2. The net beam voltage is 3,000 V as determined by the ion optical calculations. The slight decrease in beam current (15.1 mA) and as a consequence in thrust (1.37 mN) from the initial requirements is due only to the fact that, for this particular thruster, the emitting surface of the ionizer is smaller than the nominal one.

Ion Beam Characterization

During the experiments previously described, the shape of the beam was also analyzed and taken into account for the choice of the working parameters. A Faraday cup is used to measure current density profiles. It is located 70 mm downstream in the beam and is movable in two directions: along lines parallel to the ionizer and radially along circles in planes perpendicular to the ionizer.

Figure 5 shows radial profiles of the beam in three different planes perpendicular to the axis of the emitter as represented in the upper right part of the figure. A similar plot along the longitudinal direction confirms the good uniformity of the emission at the ionizer surface. The symmetry of the beam relative to both the perpendicular and longitudinal medial planes is respected and on the whole the shape is satisfactory and in agreement with the calculated one. The angle of divergence can be deduced: calculated as the angle in which passes 90% of the total current it is found to be $\pm 17°$ (to be compared to the 17.5° computed during the optical calculations).

The technique is also used to determine the deflection capabilities of the optics and Fig. 6 represents the variation of the radial profile when a differential voltage of 500 volts is applied between the two halves of the accelerator electrodes. The main results are that the deflection is effective, without deterioration of the shape of the beam. The current density remains uniform, and no measurable increase is observed on the accelerator current.

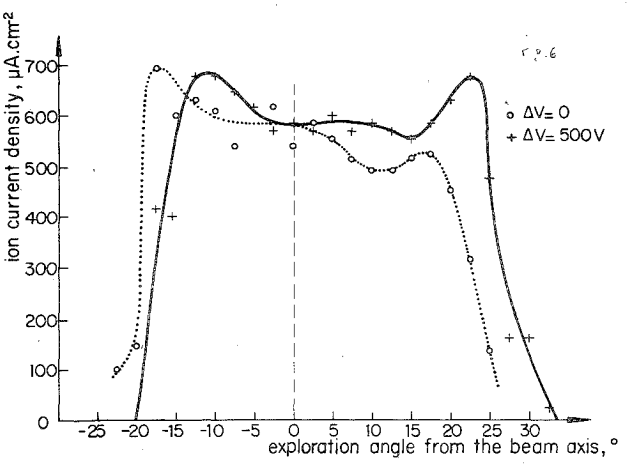

Fig. 6 Effect of the accelerator differential voltage on the radial profile of the beam.

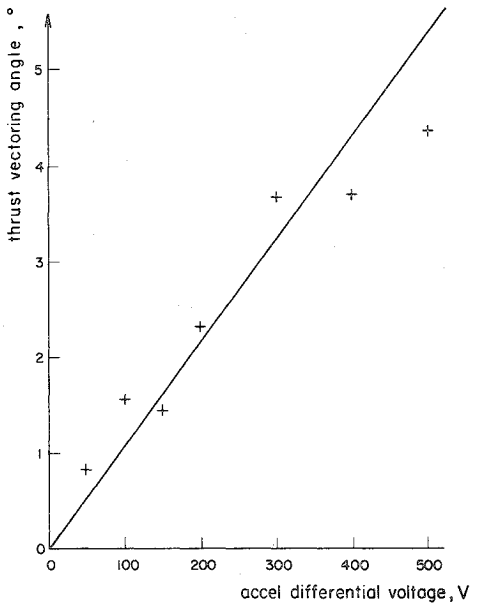

Fig. 7 Variation of the thrust vectoring angle with the differential voltage applied on the accel-electrodes.

The actual value of the thrust vectoring angle φ has been computed by integrating of the probe signal over the angle of exploration. If x is the angle between the probe axis and the ionizer axis and $f(x)$ the probe signal, then

$$\varphi = \arctan \frac{\int_{-\pi/2}^{+\pi/2} f(x) \sin x dx}{\int_{-\pi/2}^{+\pi/2} f(x) \cos x dx} \quad (1)$$

It is plotted Fig. 7 against the applied differential voltage.

Drain Currents on the Accelerator Electrodes

Among the main difficulties encountered with a thruster using cesium as propellant, the leaks at the accelerator level are perhaps the most serious.[8] From Table 2, one can see that in our case, drain currents of about 1.5 mA are present. They cause loss in power efficiency and they also limit the life-time and the long term reliability of the motor.

The different possible causes of leakage can be listed: 1) surface currents along the insulators when they are covered by cesium; 2) primary ions striking the "accel" electrodes, due to a wrong choice in the parameters of the optics; 3) secondary ions due to ionization or charge exchange between the residual neutral cesium flow and the primary ions; 4) electron emission

due to a) field emission, strongly dependant on the smoothness of the surface of the accelerator electrodes; b) thermionic emission, very sensitive to the adsorbed cesium layer on these elctrodes.

To study these losses, an experimental program was developed based on the comparison between two regimes of the ion source. The first is the nominal one, at normal beam current and electrodes voltages. The second regime is chosen to simulate the nominal regime while suppressing the ion beam by decreasing the ionizer temperature below its critical value. This simulated regime serves to separate the effects of the neutrals from those of the primary and secondary ions. The high voltages are maintained and neutral effluxes equivalent to the ones present in the normal regime are created by proper selection of the cesium feed rate.

By definition of the propellant efficiency, the neutral efflux is equivalent to a current: $I_{\text{neutral}} = (1-\eta_u)\ I_{\text{beam}}$. For the experiments in the simulated regime: $\tau^* = 1-\eta_u = 0.5$ to 1%.

A way to adjust the neutral flow to the chosen value of τ is to measure the corresponding ion current obtained by an increase of the ionizer temperature well above its critical value. The similitude between the neutral flux distribution in the two regimes has been controlled using a neutral detector.

The different causes of parasitic currents can then be analysed: 1a) *Surface currents on the isolators:* by working in the simulated regime and applying only one of the two high voltages, one can place separately the insulators in conditions similar to their normal environment since all the local conditions (electric fields, vapor pressure) are respected. The currents flowing to the base plate are found to be negligible (in the microampere range) and this first cause can be eliminated. This result is consistent with the precautions taken for the location and design of the insulators.

2) *Interception of the primary ions:* an interception of the accelerator electrode by the primary ions was improbable because of the good agreement between the experimental beam profiles and the computed trajectories. This is confirmed by the fact that in the nominal regime the beam current can be modified in a few seconds by changing the high voltages while a corresponding change in accelerator currents has a time constant of about 20 min.

3) *Collections of secondary ions:* two heaters were installed inside the accelerator electrodes in order to control their temperature independently of the radiation from the ionizer. Figure 8 shows the variation of the accelerator current with the temperature of the electrodes in the nominal regime and in the simulated regime for different values of the neutral flow. The role of the secondary ions can be eliminated since the same order of magnitude and the same kind of variation is observed for the currents in the two regimes.

4) *The drain current is an electron emission from the cesiated accelerator electrodes:* as seen in Fig. 8, a decrease in the neutral efflux in the simulated regime results in a decrease in the drain current. The same variation is obtained by an increase of the accelerator temperature. These variations take place with long time constants and are evidently related to a change in the surface coverage conditions and the associated work function.

The curves of Fig. 9 are obtained in experimental conditions which are similar to those of Fig. 8, but nevertheless the accelerator currents, while following the same laws of variation, are much higher. This seems a confirmation of the considerable role of the surface coverage in the emission process (a slight difference in the geometry or in the experimental procedure is probably at the origin of the change in coverage and thus in work function). Among the most likely causes for these currents, two appear to be dominant: the cold emission process for which the emitted current density can be written

$$J = \alpha \frac{E^2}{\Phi} \exp\left(-\frac{\phi^{3/2}}{E}\right) \qquad (2)$$

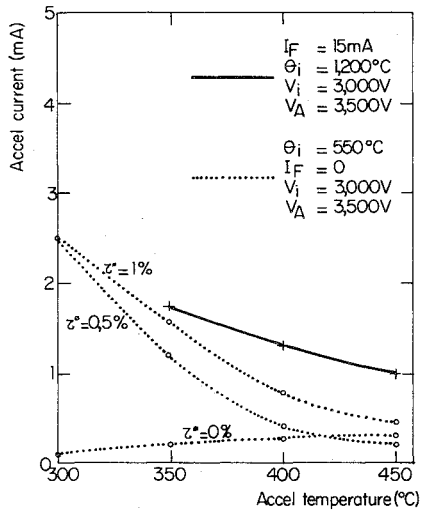

Fig. 8 Drain currents with and without ion beam for different values of the neutral flow.

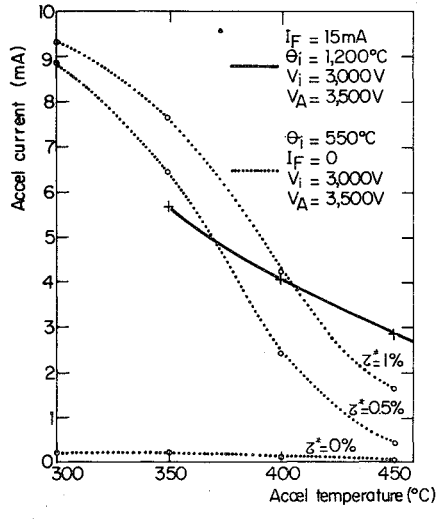

Fig. 9 Drain currents with and without ion beam for different values of the neutral flow.

and the thermoionic emission enhanced by the presence of a high electric field (Schottky effect)

$$J = A T^2 \exp - \left[\frac{e\phi}{k\theta u} \quad \frac{e(e/4\pi\epsilon_0)^{1/2} E^{1/2}}{k\theta a} \right]^{1/2} \qquad (3)$$

In the latter case, it is impossible to correlate directly the formule to the experimental measurements since a change in the temperature θa of the electrode is followed by a change in the work function ϕ. It is also impossible to study in the normal regime the variation of J with the electric field since any variation in the voltages leads to important changes in the ion source performances. On the contrary, the role of the electric field can be analyzed in the simulated regime. The flow of neutrals and the temperature of the electrodes, thus the work function, can be held constant while the fields are varied. Figure 10 gives a plot of Log $(I_A/E^2) = f(1/E)$ on which a straight line is representative of a cold emission process (formule 1). To obtain a straight line in the enhanced thermoionic emission (formule 2), one can plot the curve of Fig. 11: Log $I_A = f(V^{1/2})$.

The working conditions correspond to the point A on the two figures. The experimental points of Fig. 11 are practically aligned, a result which would be favorable to enhanced thermoemission if the slope of the curve was not so steep. The anomalous Schottky effect[7] can explain a steeper slope and may be present in the observed phenomenon. For the high

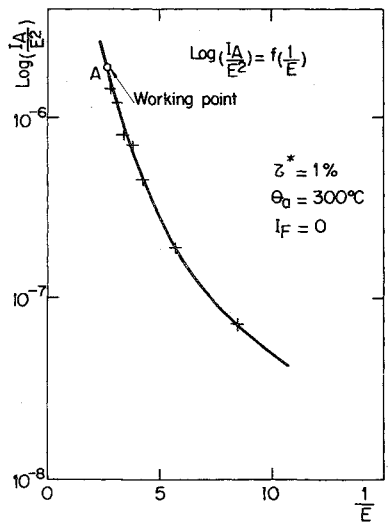

Fig. 10 Experimental research of a field emission process.

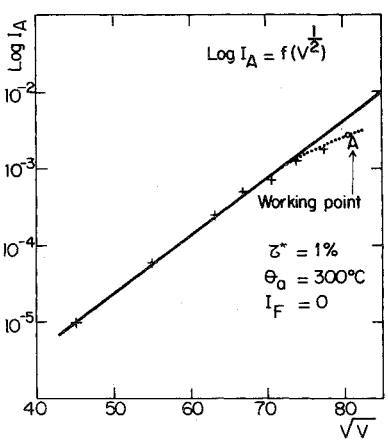

Fig. 11 Experimental research of the Schottky effect.

electric fields, and particularly at the working point, the cold emission process seems the more likely.

As a conclusion of these experiments, the field emission of electrons from the accelerating electrode is greatly dominant compared to the surface currents on insulators and ion interception. An increase around 600°C of the temperature of the accelerating electrode has been shown effective to reduce the drain currents to negligible values. One way this temperature can probably be obtained is by changing the design of the electrode.

Conclusions

An engineering model of the cesium contact ion thruster has been developed and tested successfully. The analysis of the performances of the main components have shown that the long lifetime and the reliability necessary for a space application can be expected and on the whole the thruster is now ready for endurance tests and industrial development. The experiments have shown that, through the control of the temperature and surface smoothness of the accelerator electrodes, the electron current which is still present in our case should be reduced to negligible levels.

References

[1] Brewer, G.R., *Ion Propulsion,* Gordon and Breach, 1970.

[2] Le Grives, E., et al., "A Linear Strip Cesium Contact Ion Thruster for Aixiliary Propulsion," AIAA Paper 75-415, Anaheim, Calif. 1975.

[3] "La Propulsion Electrique a Ionisation de Cesium par Contact," *Acta Electronica,* Vol. 17, Oct. 1974.

[4] Eschard, G., et al., "Basic Studies of a Cesium Contact Ion Thruster," AIAA Paper 72-440, Bethesda, Md., April 1972.

[5] Eschard, G., et al., "The Engineering Model of a Cesium Contact Ion Thruster," 2nd European Electric Propulsion
Culham (G.B.), April 1973.

[6] Le Grives, E. and Labbe, J., "French Research on Cesium Contact Ion Sources," *Journal of Spacecraft and Rockets,* Vol. 10, Feb. 1973, pp. 113-118.

[7] Eschard, G., et al., "Development and Experimentation of a Cesium Contact Ion Thruster," 3rd European Electric Propulsion Conference, Hinterzarten (FDR), October 1974.

[8] Moore, D. and Forrester, A.T., "Accelerator Electrode Currents in Ion Engines," *AIAA Journal,* Vol. 3, Nov. 1965, p. 2013.